Processing and Application of Ceramics 12 [2] (2018) 118–122
https://doi.org/10.2298/PAC1802118O

TiO_2 ceramics prepared using Pechini synthesis and laser sintering

Tiago Cordeiro Oliveira*, Emanuel Ferreira Silva

Federal Institute of Sergipe, Brasil

Received 25 January 2018; Received in revised form 11 March 2018; Accepted 9 May 2018

Abstract

Nowadays, the laser sintering process has attracted the attention of researchers owing to advantages such as the possibility of using very high heating and cooling rates and the possibility of sintering materials with high melting point. TiO_2 ceramics was produced from powders synthesized using the polymer precursor method. The purpose of this paper was the sintering of TiO_2 samples using an unconventional method with CO_2 laser as the heating source. Techniques such as differential thermal analysis, thermogravimetry, X-ray diffraction, scanning electron microscopy, and impedance spectroscopy were used for the sample characterizations. The sintering time was extremely fast, around 3 minutes. Moreover, the samples showed lower resistivity when compared to those sintered conventionally.

Keywords: *Pechini method, rutile, sintering, CO_2 laser*

I. Introduction

The physical properties of a material depend intrinsically on its constituents and defect structure. However, in ceramic materials, there is a significant dependence of these properties on the microstructure, which is closely related to the sintering process and the characteristics of the precursor powders. Thus, the understanding of the sintering process is of immense scientific and technological importance for the development of ceramics with new and improved properties [1,2]. Sintering is traditionally performed using an electric furnace. However, alternative techniques such as microwave sintering, hot isostatic pressing, spark plasma sintering, and laser radiation of CO_2 have also been used [3,4]. The laser sintering technique will be presented and discussed in this paper.

The first study about the emission of CO_2 laser was undertaken in 1964 by Patel *et al.* [5] and subsequently, the use of CO_2 laser in the processing of materials has been well studied. The first paper on the sintering of ceramic bodies using a CO_2 laser was presented in 1984 by Okutomi *et al.* [6]. The main advantages of this technique are its high processing speed, localized heating, the possibility of using high rates of heating and cooling, no use of a crucible container, reduction of the chances of contamination, and the possibility of sintering materials with high melting point [6,7].

In the laser-matter interaction, the energy is absorbed and transformed into heat. Owing to its high temperature gradients, high heating rates, superficial quickness of the process and the absorption of energy, the ceramics sintered using a laser can exhibit different characteristics when compared to the ceramics sintered using the conventional method. In recent years, some authors have reported and compared the properties of laser-sintered ceramics with the conventional method in materials such as SnO_2, Al_2O_3-WO_3, Ta_2O_5, SiO_2, $Bi_4Ti_3O_{12}$, $Bi_4Ge_3O_{12}$, $BaTiO_3$, $Ba_{1-x}Ca_xTiO_3$, $K_{0.5}Na_{0.5}NbO_3$ [7–15].

TiO_2 has numerous properties and applications of technological interest, such as anticorrosive devices, photovoltaic cells, solar protectors, photocatalysts, gas sensors, and humidity sensors, and it is also used as a white pigment in the industry. TiO_2 has three crystalline forms: rutile, anatase, and brookite. The rutile phase has various applications in the electronics industry in devices such as capacitors and varistors. The brookite and anatase phases transform irreversibly to rutile after heating above 700 °C [16–18]. In this work, TiO_2 oxides were produced using the polymer precursor method and then sintered by CO_2 laser, a sintering method that is very fast and scarcely reported in the scientific literature. The optimized conditions for the sintering of these oxides were determined during the laser sintering and they were compared with the samples sintered using an electrical furnace.

* Corresponding author: tel: +55 7937111400,
e-mail: *tiagocordeirotc@yahoo.com.br*

II. Experimental procedure

In this paper, TiO_2 powders were synthesized using the Pechini method, also known as the polymer precursor method, which is based on the formation of a polymer in which metal ions are incorporated. This method was used because it presents advantages such as high purity, good chemical homogeneity, low implantation cost, synthesis at low temperatures, and the possibility of obtaining powders with lower grain size [19,20]. The reagents used to obtain the powders are listed in Table 1. Citric acid (CA) was initially dissolved in distilled water in concentration of 0.6 g/ml. After complete homogenization, a metal ion precursor was added in the molar ratio of citric acid: metal ion of 6 : 1, and the solution was maintained at a constant temperature of approximately 70 °C. After homogenization of the solution, ethylene glycol (EG) was added in the mass ratio of 3 : 2 (CA : EG), and the temperature was increased to 120 °C. All the steps were performed under stirring. For the production of powders, the solutions were calcined at 600 °C for 4 h at the heating rate of 2 °C/min.

For the sintering, the calcined powders were mixed with an aqueous solution of polyvinyl alcohol (0.1 g/ml) and thereafter moulded via uniaxial pressing into cylindrical ceramic bodies of 1.2 mm thickness with diameter 4 mm. The experimental procedure for laser sintering entailed maintaining the laser beam fixed on the central point of the sample by linearly varying the power density incident on the sample. The beam of laser emerging from the source was reflected by a series of mirrors and was expanded using a plano-convex lens of ZnSe. In the assembled system, the sample was positioned beyond the focal point of the lens, such that it was possible to control the diameter of the laser beam incident on the sample. In the experimental apparatus, different distances between the lens and sample were adjusted, and different nominal powers of the laser radiation source were employed to obtain varying power densities. The optimization conditions of the process are described as follows. Before irradiation, the samples were placed on a base made of the same material at 300 °C in order to reduce the initial thermal gradient in the sample. This temperature was maintained throughout the sintering process. Subsequently, the power density was increased at a linear rate of 2.0 W/mm^2·min to the maximum value of power density (P_{max}) and maintained for 45 s. After irradiation of the first face, the sample was turned and the procedure was repeated on the other side of the sample. Under these conditions, the entire sintering process lasted for approximately 3 min, which is significantly faster than the conventional sintering process in an electrical furnace. Figure 1 shows the schematic of the experimental apparatus used in the laser sintering process.

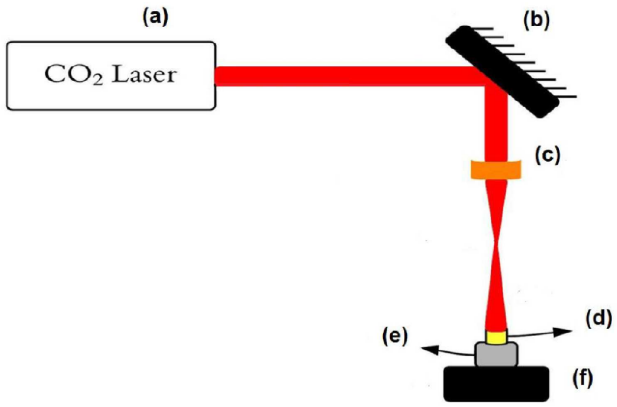

Figure 1. Scheme of the experimental apparatus used for sintering with laser radiation: a) laser radiation source, b) mirror, c) ZnSe lens, d) sample, e) base made of the same material as the sample, f) furnace maintained at 300 °C

The differential thermal analysis (DTA) and thermogravimetry (TG) measurements were performed simultaneously in the temperature range from 25 to 1300 °C at the heating rate of 10 °C/min in an atmosphere of synthetic air ($O_{2/}N_2$ - 1/4) with alumina as the reference material. The measurements were performed in the Nerzsch STA 409 equipment using TiO_2 precursor resin dried at 100 °C for 24 h.

X-ray diffraction (XRD) measurements were performed using a Rigaku RINT 2000/PC diffractometer with CuKα radiation in the 2θ range from 20 to 80° in the continuous scan mode at steps of 2° per minute.

The microstructure of the sintered samples (without previous thermal, chemical, or polishing treatment) was examined using scanning electron microscopy (SEM, JEOL, JSM-6510LV). The average grain size was estimated from the SEM images using the intercepts method, according to ASTM standards.

The sintered samples for the impedance spectroscopy measurements were previously polished with water sandpaper and cleaned using a bath ultrasonic device. After cleaning, the faces were painted with platinum paint and heated at 700 °C for 30 min to remove the solvent and crystallize the electrodes. Electrical measurements were performed using the Solatron 1260 impedance analyser under the following conditions: isothermally applying a potential of 1 V and varying the excitation frequency in the range of 1 Hz to 10 MHz.

Table 1. List of precursors used in the preparation of the powders

Name	Chemical formula	Purity [%]	Manufacturer
Citric acid	$C_6H_8O_7$	99.5	Vetec
Ethylene glycol	$HOCH_3CH_2OH$	99	Synth
Titanium isopropoxide	$Ti[OCH(CH_3)_2]_4$	97	Alfa Aesar

III. Results and discussion

Figure 2 shows the DTA/TG curves of the TiO_2 precursor resin dried at 100 °C for 24 h. In the synthesis using the Pechini method, the reactions at temperatures lower than approximately 450 °C are mainly dependent on the precursors, whereas the main combustion reaction commonly occurs between 450 and 600 °C [19]. The crystalline phase is formed in this temperature range, and for the TiO_2 precursor resin this was 570 °C (Fig. 1). This temperature serves as an indication of the minimal calcination temperature of the precursor powders. Therefore, based on these results, the calcination treatment at 600 °C for 4 h was used.

Figure 3 shows the XRD pattern of the calcined TiO_2 powder produced using the Pechini method. The pattern was indexed according to the Inorganic Crystal Structure Database. Two phases were detected: the major anatase phase and the rutile phase in lower quantity. The predominance of the anatase phase is expected because a low-temperature synthesis method was used, favouring its stability [21]. Figure 4 shows the XRD patterns of the TiO_2 ceramics sintered conventionally at 1350 °C/6 h and using a laser at 1.6 W/mm^2 for 45 s. In both cases, only the formation of a rutile phase was observed, this behaviour was expected owing to the anatase/rutile phase transition at high temperatures [17,18].

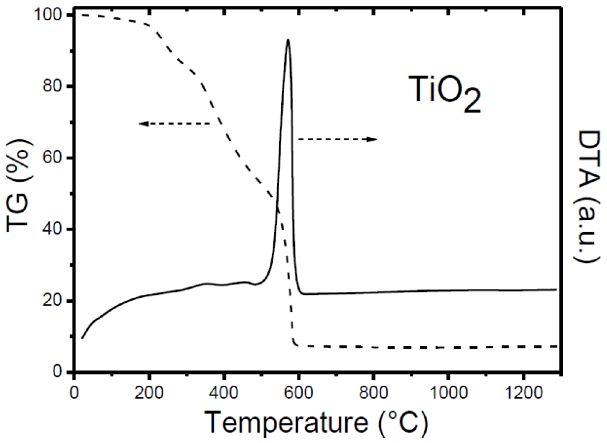

Figure 2. DTA/TG curves of the precursor resin after drying for 24 h at 100 °C

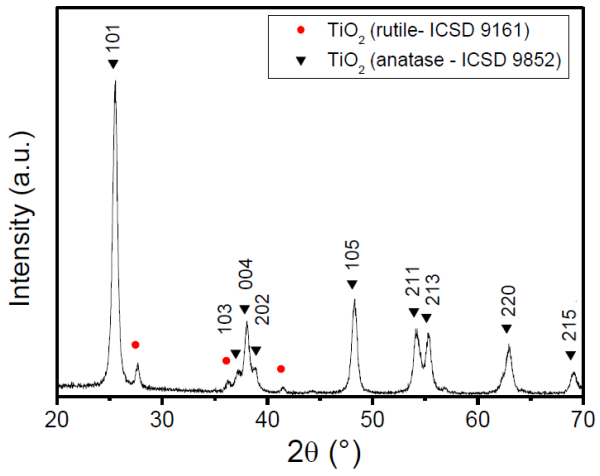

Figure 3. X-ray diffraction pattern of TiO_2 powder calcined at 600 °C for 4 h

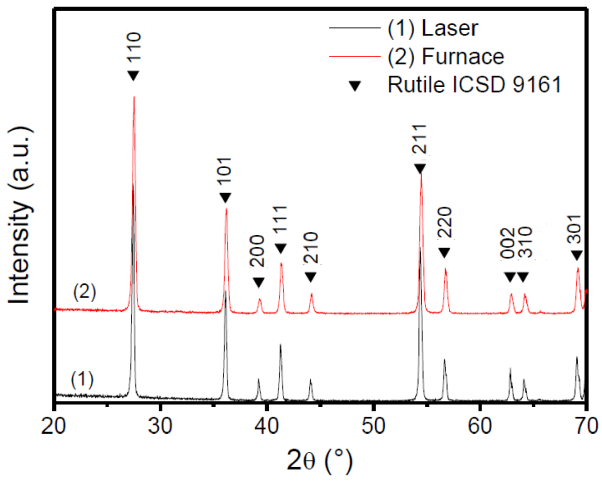

Figure 4. X-ray diffraction pattern of TiO_2 ceramics sintered conventionally in furnace and by laser

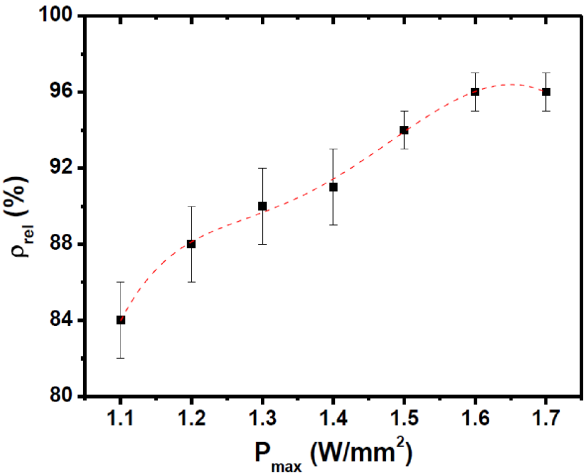

Figure 5. Relative density as a function of power density (dotted line is only a guide to the eyes)

An important parameter during laser sintering is the surface power density, which reaches on the sample. This parameter is directly related to the temperature to be reached. Figure 5 shows the relative density curves (calculated using the Archimedes method) as a function of the power density (P_{max}) during laser sintering of the studied samples. For each point, the relative density (ρ_{rel}) was measured for at least three samples. For TiO_2 ceramics, the maximum relative density achieved was approximately 96% TD at the power density of 1.6 W/mm^2.

In order to verify the homogeneity between the centre and the edge of the ceramic surface, these two regions were examined using SEM. Figure 6 shows the SEM images of the surface at the central and the edge regions.

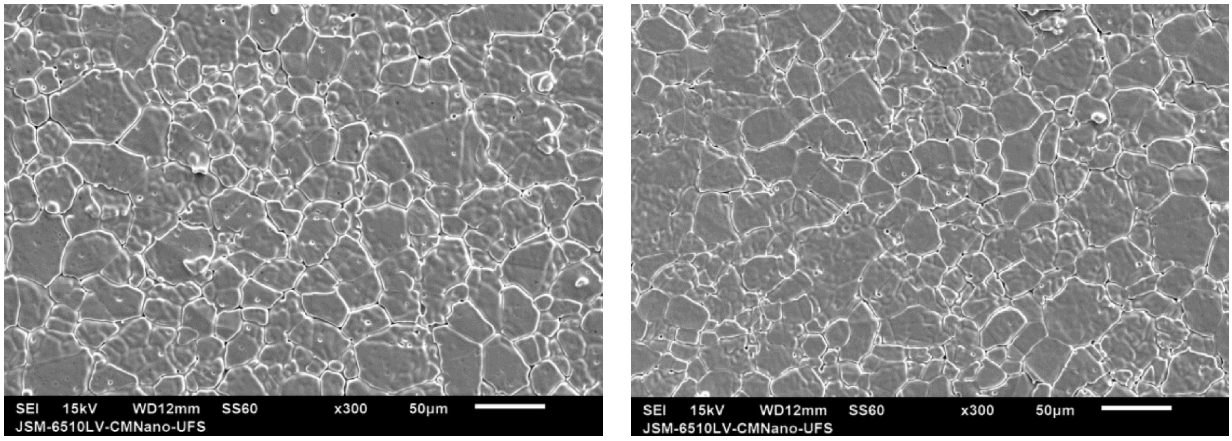

(a) (b)

Figure 6. SEM images of the surface of ceramics sintered with a laser at the power density of 1.6 W/mm^2 in: a) central and b) edge region

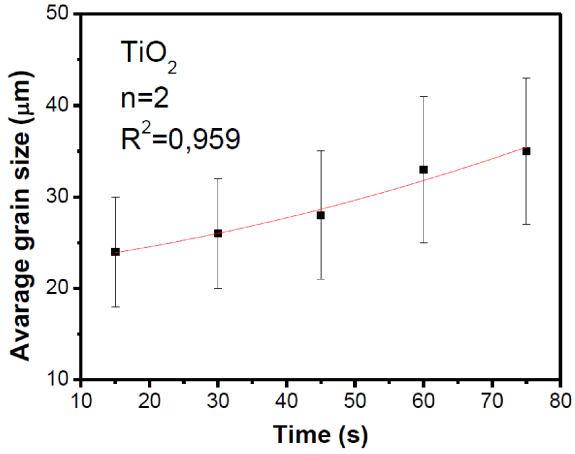

Figure 7. Isothermal curve for grain growth

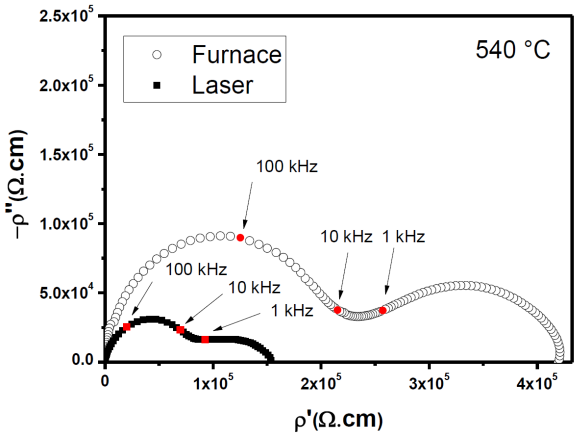

Figure 8. Impedance diagram in the complex plane for TiO_2 samples conventionally sintered in the furnace and with a laser

It can be observed that there is a good microstructural homogeneity and the average grain size was estimated to be 28 ± 8 µm. The analysis of grain size homogeneity between centre and edge region is important due to the radial temperature gradient, with higher temperatures in the centre of the sample due to the Gaussian profile of the heating that is typical for the incidence of laser radiation in ceramics. Several experimental tests were performed to obtain optimized conditions of power density, sintering time and sample size. The homogeneity was observed for different samples and different regions of these samples using the optimized conditions.

Grain growth models generally consider the shape and movement of the boundaries. The rate of movement of the boundaries is directly proportional to the curvature and, therefore, inversely proportional to the grain size (G). Considering t as the sintering time, we have:

$$\frac{dG}{dt} \propto \frac{1}{G} \tag{1}$$

By integration of Eq. 1, we obtain:

$$G^2 - G_0^2 = k \cdot t \tag{2}$$

In this equation, G_0 is the grain size at initial time and k is the proportionality constant that depends on the mobility of the boundary and the temperature. In practice, there are other exponents besides 2, but this concept was used for the following phenomenological equation:

$$G^n - G_0^n = k \cdot t \tag{3}$$

where n represents the sintering mechanism: $n = 2$ for diffusion along the grain boundary; $n = 3$ for volumetric diffusion or liquid phase; and $n = 4$ for surface diffusion.

Figure 7 presents the isothermal grain growth curves for the final stage of sintering, adjusted by the method of least squares according to Eq. 3 [22]. The value of the parameter $n = 2$ was the best for fitting the equation. This value is related to the mass transport mechanism by diffusion through the grain boundary. In the graph, R^2 is the reliability coefficient of the fit and the closer it is to 1, the better is the fit quality.

Figure 8 shows the resistivity diagrams in the complex plane for the samples sintered using the two tech-

niques. The low-frequency semicircles are associated to the grain boundary and the high-frequency semicircles are associated to the grain [23]. From the analysis of these diagrams, it can be observed that the laser sintered ceramics has a lower resistivity and thus higher conductivity. It is known that the conductive processes (electronic conduction) can increase the dielectric constant owing to the accumulation of charges on the interfaces. This behaviour may be related to the microstructural change or the presence of different defects in the two samples, as there is practically no difference in the relative densities of the samples (in both case ρ_{rel} = 94 ± 1% TD), nor in the initial chemical compositions.

IV. Conclusions

Polycrystalline TiO_2 powders were successfully produced using the polymer precursor method. By analysing the DTA/TG results, the calcination conditions were determined to be 600 °C for 4 h. The XRD measurements indicated in anatase phase as a major one in the calcined powder. The powders were sintered using a very rapid laser sintering method when compared with conventional sintering using an electrical furnace. The conditions for the laser sintering process were well-defined, and the obtained ceramics has rutile phase, relative density of ~96% TD and good microstructural homogeneity between the centre and the edge regions. The laser sintered samples also showed a lower resistivity value compared with the conventionally sintered samples.

Acknowledgement: The author thanks the UFS by the use of laboratories and CNPq for the financial support.

References

1. S.L. Kang, *Sintering: Densification, Grain Growth, and Microstructure*, Elsevier, Oxford-UK, 2005.
2. M.N. Rahaman, *Ceramic Processing and Sintering*, Marcel Decker, New York-USA, 2003.
3. R.R. Menezes, P.M. Souto, R.H.G.A. Kiminan, "Microwave sintering of ceramics. Part II: Sintering of ZnO-CuO varistors, ferrite and porcelain bodies", *Cerâmica*, **53** (2007) 108–115.
4. V. Trombini, E.M.J.A. Pallone, Z.A. Munir, R. Tomasi, "Spark plasma sintering (SPS) of Al_2O_3-ZrO_2 nanocomposites", *Cerâmica*, **53** (2007) 62–67.
5. C.K.N. Patel, "Selective excitation through vibrational energy transfer and optical maser action in N_2-CO_2", *Phys. Rev. Lett.*, **13** (1964) 617–619.
6. M. Okutomi, M. Kasamatsu, K. Tsukamoto, S. Shiratori, F. Uchiyama, "Sintering of new oxide ceramics using a high power cw CO_2 laser", *Appl. Phys. Lett.*, **44** (1984) 1132–1134.
7. R.S. Silva, A.C. Hernandes, "Laser sintering of $BaTiO_3$ ceramics obtained from nanometric powders", *Mater. Sci. Forum*, **514** (2006) 1216–1220.
8. D. Ganz, G. Gasparro, M.A. Aegerter, "Laser sintering of SnO_2:Sb sol-gel coatings", *J. Sol-Gel Sci. Technol.*, **13** (1998) 961–967.
9. F. Zheng, R. Yuan, X. Li, Z. Li, X. Tao, Q. Zheng, C.G. Zhan, "Electrical properties of laser-synthesized aluminum oxide - tungsten oxide ceramics", *J. Am. Ceram. Soc.*, **81** (1998) 2443–2448.
10. L. Ji, Y. Jiang, "Laser sintering of transparent Ta_2O_5 dielectric ceramics", *Mater. Lett.*, **60** (2006) 1502–1504.
11. N.K. Tolochko, M.K. Arshinov , K.I. Arshinov, A.V. Ragulya, "Laser sintering of SiO_2 powder compacts", *Powder Metal. Metal Ceram.*, **43** (2004) 10–16.
12. Z.S. Macedo, M.H. Lente , J.A. Eiras, A.C. Hernandes, "Dielectric and ferroelectric properties of $Bi_4Ti_3O_{12}$ ceramics produced by a laser sintering method", *J. Phys. Condensed Matter*, **16** (2004) 2811–2818.
13. Z.S. Macedo, R.S. Silva, M.E.G. Valerio, A.C. Hernandes, "Radiation detectors based on laser sintered $Bi_4Ge_3O_{12}$ ceramics", *Nucl. Instrum. Meth. Phys. Res.*, **218** (2004) 153–157.
14. X. Tian, A. Dittmar, J. Melcher, J.G. Heinrich, "Sinterability studies on $K_{0.5}Na_{0.5}NbO_3$ using laser as energy source", *Appl. Surf. Sci.*, **256** (2010) 5918–5923.
15. T.C. Oliveira, M.S. Silva, L.M. Jesus, D.V. Sampaio, J.C.A. Santos, N.R.S. Souza, R.S. Silva, "Laser sintering and radioluminescence emission of pure and doped Y_2O_3 ceramics", *Ceram. Int.*, **40** (2014) 16209–16212.
16. Y. Liu, A.R. West, "Semiconductor-insulator transition in undoped rutile, TiO_2, ceramics", *J. Am. Ceram. Soc.*, **96** (2013) 218–222.
17. S.J. Webb, L.F. Cohen, N.McN. Alford, "Microwave dielectric loss of titanium oxide", *J. Am. Ceram. Soc.*, **83** (2000) 95–100.
18. L. Castañeda, J.C. Alonso, A. Ortiz, E. Andrade, J.M. Saniger, J.G. Bañuelos, "Spray pyrolysis deposition and characterization of titanium oxide thin film", *Mater. Chem. Phys.*, **77** (2003) 938–944.
19. R.S. Silva, M.I.B. Bernardi, A.C. Hernandes, "Synthesis of non-agglomerated $Ba_{0.77}Ca_{0.23}TiO_3$ nanopowders by a modified polymeric precursor method", *J. Sol-Gel Sci. Technol.*, **42** (2007) 173–179.
20. T.W. Li, S.Q. Yang, S. Li, "Preparation and characterisation of perovskite $La_{0.8}Sr_{0.2}Ga_{0.83}Mg_{0.17}O_{2.815}$ electrolyte using a poly(vinyl alcohol) polymeric method", *J. Adv. Ceram.*, **5** (2016) 167–175.
21. B.R. Sankapal, M.C. Lux-Steiner, A. Ennaoui, "Synthesis and characterization of anatase-TiO_2 thin films", *Appl. Surf. Sci.*, **239** (2005) 165–170.
22. R. Chaim, A. Shlayer, C. Estournes, "Densification of nanocrystalline Y_2O_3 ceramic powder sintering", *J. Eur. Ceram. Soc.*, **29** (2009) 91–98.
23. J.R. Macdonald, *Impedance Spectroscopy: Emphasizing in Solid State Materials and Systems*, John Wiley, New York-USA, 1987.